

# Effect of Nanocalcium Carbonate Content on the Properties of PLA Nanocomposites

Ankit Pundir<sup>1</sup>, P. Santhana Gopala Krishnan<sup>1,\*</sup> and Sanjay Kumar Nayak<sup>1,2</sup>

<sup>1</sup>Department of Plastics Engineering, Central Institute of Plastics Engineering and Technology, Patia, Bhubaneswar-751024, India

<sup>2</sup>Laboratory for Advanced Research in Polymeric Materials, Central Institute of Plastics Engineering and Technology, Patia, Bhubaneswar-751024, India

**Abstract:** Even though poly(lactic acid) is one of the most promising biodegradable polymers, less hydrophilic, low impact strength and heat resistance limits its applications. The current study was undertaken to overcome these limitations. Poly(lactic acid)-calcium carbonate nanocomposites were prepared by melt blending technique upto 3 wt. % using master batch containing 4 wt. % of nanocalcium carbonate content. Water absorption and density increased with increase in nanofiller content. Tensile and flexural strength and heat deflection temperature increased up to 1 wt. % of nanofiller content and marginally decreased thereafter. Impact strength increased with increase in nanofiller content and was attributed to cavitation at the polymer-particle boundaries. Impact strength increased to about 200% upon addition of 3 wt. % of nanofiller. TEM studies indicated good dispersion of nanofiller at 1 wt. % and agglomeration at 3 wt. % of nanofiller content. Nanocomposites had lower thermal stability than pristine polymer.

**Keywords:** Poly(lactic acid), nanofiller, mechanical properties, thermal stability.

## 1. INTRODUCTION

Poly(lactic acid) (PLA) is one of the most promising commercially available biodegradable aliphatic polyesters because of its low fossil energy requirement and greenhouse gas emission when compared to petroleum based plastics [1-6]. 50 millions of 27g PLA bottles save 13,600 barrels of crude oil and electricity required for 40,000 people for a period of one month [7]. The net greenhouse gas emission for one kg of PLA is 0.3kg of carbon dioxide equivalence whereas for PP, PET, PC and nylon are 1.9, 3.4, 7.6 and 7.9kg respectively [8]. Literature search indicated that PLA could be toughened through blending with various polymers namely poly(butylene succinate) [9], poly( $\epsilon$ -caprolactone) [10], poly(ethylene glycol) [11], poly(vinyl alcohol) [12]. It has been reported that synthetic elastomers such as isoprene rubber, acrylonitrile-butadiene rubber, ethylene-acrylic rubber, ethylene-propylene copolymer could be melt blended to toughen PLA [13]. Balakrishnan *et al*, [14] has studied mechanical, thermal and morphological properties of LLDPE toughened PLA nanocomposites. LLDPE was found to improve the impact strength of PLA nanocomposites at the expense of tensile and flexural strength. Alternatively, the use of plasticizers such as poly(ethylene glycol) [15], poly(propylene glycol) [16], oligomeric lactic acid [17], glycerol [18], citrate ester

[18], diethyl bis(hydroxymethyl) malonate oligomers [19], triacetine [19, 20], tributyl citrate [19, 21], partial fatty acid ester [22], has been studied to improve the impact strength of PLA. Plasticization had significantly improved the elongation<sub>365</sub> at break and impact strength of PLA but the inherent stiffness of PLA was sacrificed [22], thereby making it undesirable for structural applications.

Another way of improving the desirable properties such as tensile strength and modulus, flexural strength and modulus and toughness is by the addition of inorganic fillers into polymer matrix. The reinforcing efficiency of fillers and ease of dispersion in the polymer matrix depend on its chemical composition, particle size and geometry. In the past few decades, intensive research efforts have been carried out on the development of nanocomposites to achieve the required level of performance at low weight fractions. The properties of micron sized particulate composites are inferior to that of nanosized fillers for the same level of filler content. This provides opportunities for material scientists to develop newer nanocomposite materials having improved structural and functional properties. Several studies have been reported on the use of fillers for reinforcement of PLA. Shibata *et al*, [23] prepared PLA-organoclay nanocomposites by melt compounding in the presence of plasticizer and reported improvement in mechanical properties of PLA. Significant improvement in tensile strength and modulus and elongation at break was reported by Hasook *et al*, [24] on addition of clay in PLA matrix.

\*Address correspondence to this author at the Department of Plastics Engineering, Central Institute of Plastics Engineering and Technology, Patia, Bhubaneswar-751024, India; Tel: +91-674-2743767, +91-9337476507; Fax: +91-674-2743863; E-mail: psgkrishnan@hotmail.com

Improved thermal, mechanical and impact properties were reported for PLA–calcium sulphate composites [25].

Jiang *et al*, [26] has studied toughening of PLA using cubic shaped nanoCaCO<sub>3</sub> and montmorillonite clay. They reported that the increase in strain-at-break was due to massive crazing in the case of cubic shaped nanoCaCO<sub>3</sub> and due to shear yielding in the case of montmorillonite clay. Liang *et al*, [27] reported the crystalline properties of PLA filled with nanoCaCO<sub>3</sub>. In another study, the thermal properties of poly(l-lacide) nanocomposites [28] containing nanoCaCO<sub>3</sub> in the range of 5 to 20 wt % was studied. In the present work, spherical shaped nanoCaCO<sub>3</sub> was used as a nanofiller in PLA matrix containing both D- and L-isomers. Further, nanocomposites were known to reinforce to a greater extent at lower concentration, which was not addressed in earlier study [28]. The effect of nanoCaCO<sub>3</sub> content from 0.25 to 3.0% on the properties of PLA nanocomposites was studied to overcome the limitations of PLA such as low hydrophilicity, low impact strength and heat resistance and the results are discussed in detail.

## 2. MATERIALS AND METHODS

### 2.1. EXPERIMENTAL

#### 2.1.1. Materials

PLA pellets (Ingeo Biopolymer 3052D) having specific gravity of 1.24 and MFI of 14g / 10min at 210°C with a load of 2.16kg was generously provided by Harita Polymers Ltd, Chennai, India. Stearic acid coated nanoCaCO<sub>3</sub> was used as such and has the average particle size of 65nm.

#### 2.1.2. Nanocomposite Preparation

PLA nanocomposites were prepared by melt blending technique through master batch route. Composition details of nanocomposites are given in Table 1. PLA and nanoCaCO<sub>3</sub> were dried for 3 hours at 80°C prior to blending and then were mixed thoroughly in a high speed mixer for 2minutes at 400 rpm to get a master batch containing 4% nanoCaCO<sub>3</sub>. The mixture was then subsequently fed into co-rotating twin screw extruder (Model SP V/70 Specific Engg. and Automats Vadodara, India) for melt compounding. The barrel temperature profile adapted during the preparation of nanocomposite was 155-160°C at the feed section, 160°C at compression zone and 165°C at metering zone and die head. L:D ratio is 40:1. The barrel screw speed was maintained at 90 rpm for all runs and the

extrudate was cooled in a water bath and subsequently pelletized. Then this master batch was mixed with virgin PLA to prepare various nanocomposites as indicated above using twin screw extruder.

**Table 1: Physical Properties of PLA Nanocomposites**

Sample Code	Weight of NanoCaCO <sub>3</sub> (%)	Water Absorption (%)	HDT (°C)
NC-0	0	0.25	56
NC-0.25	0.25	0.42	58
NC-0.5	0.5	1.71	59
NC-1	1.0	3.65	64
NC-2	2.0	4.0	60
NC-3	3.0	4.2	58

#### 2.1.3. Testing and Characterization

FT-IR spectra were recorded at room temperature using Thermo Scientific Nicolet 6700 FT-IR spectrometer (Thermo Nicolet Limited, Cambridge, UK). Water absorption test was carried out according to ASTM D570 using sample size of 100 x 12.4 x 3mm. Mettler Toledo weighing balance was used to determine the density of nanocomposites as per ASTM D729 (Mettler-Toledo India Private Limited, Mumbai, India). Wide angle X-ray diffraction (WAXD) measurements were carried out using Shimadzu XRD-6000 X-ray diffractor unit with CuK radiation (40kV, 30mA) at a wavelength of 1.54 Å (Shimadzu Lab XRD-6000, Shimadzu Corporation, Tokyo, Japan).

The test specimens for mechanical properties were prepared using injection molding machine (Endura 90 Make, Electronica Plastics Machines Ltd. Kolkata, India). The pellets prepared by extrusion were dried in air oven at 80°C for 3h prior to injection molding. Barrel temperatures were set at 185, 190, 195 and 180°C from the feeding zone to the nozzle respectively and the mold temperature was 30°C and cooling time was 30s. Specimens were then conditioned at 23 ± 2°C and 50 ± 2% RH for 48 hours before testing. A minimum of five samples were tested and average was taken. Dumbbell shaped tensile specimens having a dimension of 165 x 12.7 x 3mm were tested as per ASTM D638, using Shimadzu AG-IS Universal Testing Machine (Shimadzu Corporation, Tokyo, Japan). A crosshead speed of 50mm/min and a gauge length of 50mm were used for tensile test. Universal Testing Machine (UTM) Instron 3382 100 kN (Pennsylvania, USA) was used for flexural test using a rectangular bar

of 125 x 12.4 x 3mm dimension as per ASTM D790 standard with three point bending mode. A crosshead speed of 5mm/min and a span length of 100mm were used. Impactometer 6545 (CEAST Italy) was used for impact test using a rectangular bar specimen of 63.5 x 12.7 x 6.4mm dimension with a V-notch depth of 2.54mm and notch angle of 45° as per ASTM D256 standard.

Heat deflection temperature (HDT) was measured using Davenport Instrument (West Sussex, UK) as per ASTM D648. Morphologies of nanocomposites were studied using transmission electron microscopy (TEM; JEM 1400 Jeol Japan) under an acceleration voltage of 120kV. Ultra thin sections with thickness of about 70nm for TEM observations were cut using a Cryo Leica EM UC6 microtome (Wetzlar, Germany) at RT. After microtoming, the sections were transferred on a carbon-coated 300 mesh copper grid for TEM observations. Weight loss was examined in the temperature range of 100–650°C using Perkin Elmer Pyris1 Thermo gravimetric Analyzer (TGA) (Massachusetts, USA) at a heating rate of 10°C/ min in nitrogen atmosphere with a sample size of 5 ± 1mg.

#### 2.1.4. Water Absorption

Percentage of water absorbed was determined using the following formula:

$$W = \frac{(W_f - W_i) \times 100}{W_i}$$

where  $W_f$  and  $W_i$  are the weight of sample after immersion in water and initial dried sample weight

respectively. Three samples of each composition weighing about 1g each were dried in vacuum oven at  $80 \pm 2^\circ\text{C}$  for 3h, cooled in desiccator and then immediately weighed to the nearest three decimals. The weighed samples were then immersed in double distilled water at  $30^\circ\text{C}$  for 24h. Samples were removed from water and the excess water was wiped off using dry cloth and weighed again to the nearest three decimals.

#### 2.1.5. Density Studies

Theoretical density of nanocomposites ( $\rho_{mix}$ ) were calculated using the following equation:

$$\rho_{mix} = \frac{m_{mix}}{v_{mix}} = \frac{m_{mix}}{\frac{m_1}{\rho_1} + \frac{m_2}{\rho_2}} = \frac{1}{\frac{m_1}{m_{mix}\rho_1} + \frac{m_2}{m_{mix}\rho_2}} = \frac{1}{\frac{w_1}{\rho_1} + \frac{w_2}{\rho_2}}$$

where  $\rho_1$  and  $w_1$  are the density and weight fraction of PLA respectively and  $\rho_2$  and  $w_2$  that of nanoCaCO<sub>3</sub>.

### 3. RESULTS AND DISCUSSION

#### 3.1. FT-IR

FT-IR spectra of NC-0 and NC-3 are given in Figure 1. IR absorption peaks at 3006 and 1442cm<sup>-1</sup> were due to the stretching and bending vibrations of C-H bond respectively in NC-0. In the case of NC-3, the stretching and bending vibrations of C-H bonds were observed at 2999 and 1450cm<sup>-1</sup> respectively. The carbonyl stretching peak ( $\nu_{C=O}$ ) was observed at 1749 and 1752cm<sup>-1</sup> for NC-0 and NC-3 respectively. In NC-0, C-O stretching peak was observed at 1188cm<sup>-1</sup> whereas upon addition of nanoCaCO<sub>3</sub>, the peak shifted to 1172cm<sup>-1</sup>. The shift of IR peaks in NC-3 when

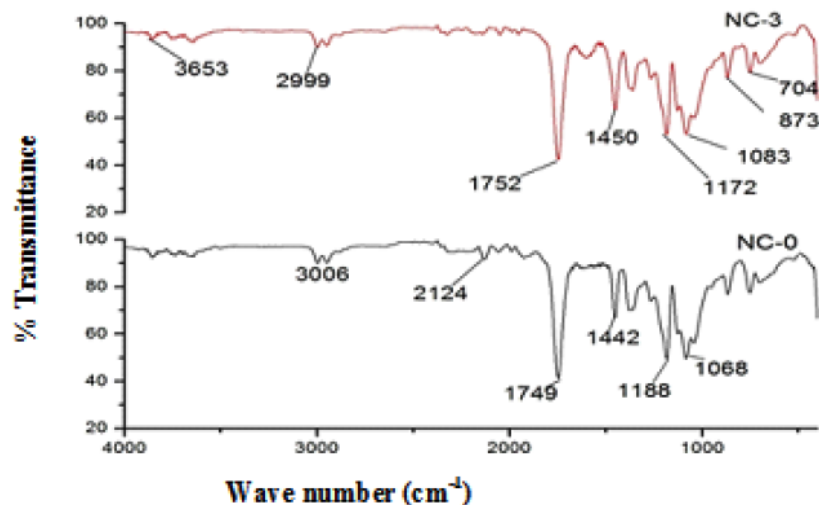


Figure 1: FT-IR spectra of PLA nanocomposites.

compared to NC-0 indicated the existence of strong interaction between nanofiller and PLA matrix. The peak at  $873\text{cm}^{-1}$  in NC-3, was assigned to carbonate of  $\text{nanoCaCO}_3$  particles.

### 3.2. Water Absorption

Table 1 shows water absorption values of nanocomposites. The values indicate that pristine PLA (NC-0) has low water absorption than nanocomposites because of the less hydrophilic nature of PLA whose reported contact angle in water was about  $74^\circ$  [29]. Water absorption increased with increase in  $\text{nanoCaCO}_3$  loading and with the introduction of 0.25, 0.5, 1, 2 and 3 wt. % of nanofiller to PLA matrix, the values enhanced by 68, 584, 1360, 1500 and 1580% respectively with respect to pristine PLA (NC-0). This was attributed to the hydrophilic nature of  $\text{nanoCaCO}_3$  in PLA matrix. In the case of poly(urethane methacrylate), the extent of increase in water absorption upon addition of 1.5 wt. of  $\text{nanoCaCO}_3$  was very nominal from 0.99 to 1.09% [30].

### 3.3. Density

Density of nanocomposites indicates the tightness of nanocomposites. Both theoretical and experimentally determined density of nanocomposites as a function of nanofiller is given in Figure 2. Density was determined theoretically using the equation. Experimentally determined density value was higher than the theoretical value which indicated that the structure of nanocomposites were in more condensed form. It has been reported that  $\text{CaCO}_3$  particles act as heterogenous nucleating agents for polymer crystallization along the interface [31]. The reason for the formation of more condensed microstructure in nanocomposites was attributed to the nucleating effect

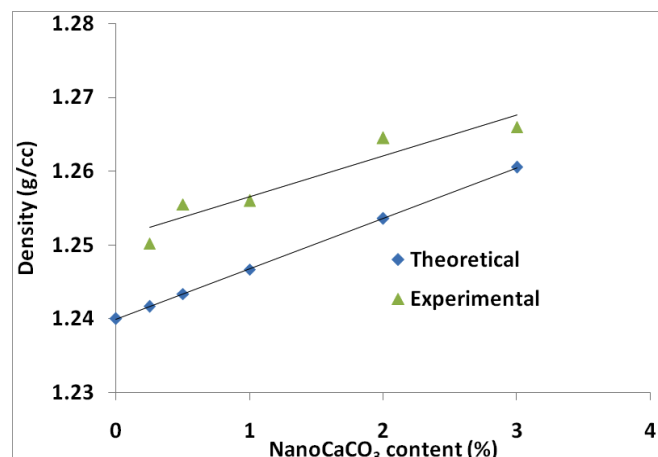


Figure 2: Plot of density vs. nano  $\text{CaCO}_3$  content.

of  $\text{nanoCaCO}_3$ . Similar observation was reported for polypropylene [32, 33].

### 3.4. Heat Distortion Temperature (HDT)

The short term thermal performance of nanocomposite materials were characterized by HDT and the values are tabulated in Table 1. HDT of nanocomposites was higher than that of pristine PLA. Increase in HDT of nanocomposites when compared to NC-0, was attributed to the presence of rigid nanofiller. HDT increased with increase in nanofiller content up to 1% i.e., NC-1 and thereafter it marginally decreased due to the agglomeration of nanofillers.

### 3.5. Wide Angle X-ray Diffraction (WAXD)

Wide angle X-ray diffraction (WAXD) pattern of NC-0 and NC-3 is given in Figure 3. Pristine PLA (NC-0) exhibited peaks at  $2\theta$  equal to  $16.8^\circ$ ,  $19.2^\circ$  and  $22.5^\circ$ . The peak at  $16.8^\circ$  was intense and assigned to (200) and / or (110) plane of orthorhombic crystal [34]. The peaks at  $19.2^\circ$  and  $22.5^\circ$  were small and assigned to the reflection from (203) and (105) planes respectively [35]. Similar peaks were observed for PLA in PLA-clay nanocomposites [36]. The presence of  $2\theta$  peak at  $29.7^\circ$  in WAXD pattern of NC-3, confirmed that  $\text{nanoCaCO}_3$  was incorporated into PLA matrix and  $\text{CaCO}_3$  is of calcite type. The absence of  $2\theta$  peak at  $26.2^\circ$  and  $38.9^\circ$  respectively suggested that  $\text{nanoCaCO}_3$  is not of aragonite and vaterite type [37].

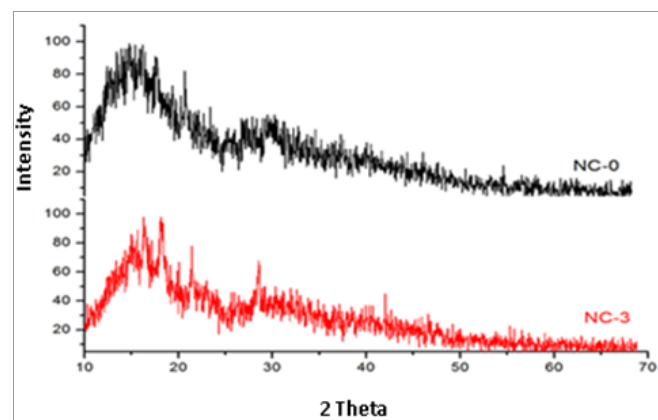
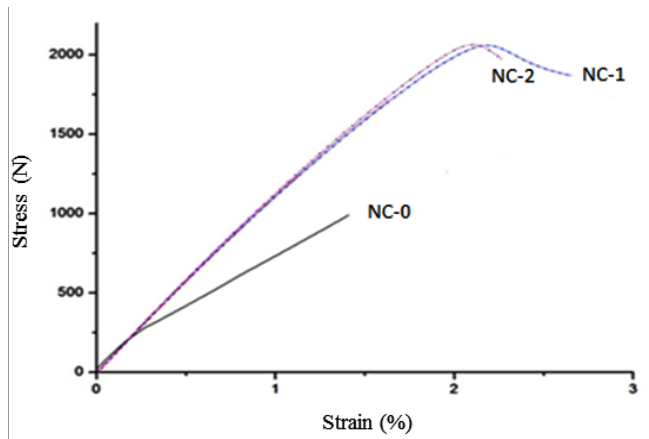


Figure 3: WAXD patterns of PLA nanocomposites.

### 3.6. Mechanical Properties of Nanocomposites

Mechanical properties of nanocomposites depend to a greater extent upon the uniform distribution of nanofiller in polymer matrix and interfacial adhesion between nanofiller and matrix and also stress distribution. Tensile stress-strain curves of nanocomposites are given in Figure 4. Tensile stress-



**Figure 4:** Stress Strain curves of PLA nanocomposites.

strain curve of pristine PLA (NC-0) indicated that the tensile stress increased with increase in strain and fracture phenomenon occurred before reaching the yield state. This indicated that the tensile failure of pristine PLA belonged to brittle fracture. The introduction of nanofiller altered the stress-strain curve and in nanocomposites, fracture phenomenon occurred after reaching the yield state, which indicated the change of fracture phenomenon from brittle to ductile. Interestingly, the stiffness of nanocomposites got enhanced with marginal increase in elongation at break. The effect of nanofiller content on tensile strength, tensile modulus and elongation at break are given in Table 2. With increase in nanoCaCO<sub>3</sub> content, tensile strength and modulus increased upto 1% of nanofiller content i.e., NC-1 and thereafter decreased. Introduction of 0.25, 0.5, 1, 2 and 3 wt. % of nanofiller to PLA matrix enhanced the tensile strength by 2.7, 41.0, 52.4, 51.8 and 31.0% and tensile modulus by 11.6, 13.3, 14.3, 13.7 and 13.0% respectively with respect to pristine PLA. Tensile properties of nanocomposites were higher than that of pristine PLA because nanoCaCO<sub>3</sub> being a rigid filler had enhanced the stiffness of PLA. Similar trend was observed in

elongation at break. Marginal increase in elongation at break was observed.

The effect of nanoCaCO<sub>3</sub> content on flexural strength is given in Table 2. The incorporation of nanoCaCO<sub>3</sub> enhanced the flexural strength up to NC-1 and decreased thereafter indicating that agglomeration had taken place in NC-2 and NC-3. For 0.25, 0.5, 1, 2 and 3 wt. % of nanofiller content, flexural strength increased by 12.3, 26.8, 69.5, 36.0 and 13.6% respectively with respect to NC-0. This behavior was due to the reinforcing effect of nanofiller in PLA matrix.

Impact strength of nanocomposites is given in Table 2. Impact strength of nanocomposites increased with increase in nanofiller content. WAXD studies indicated the nucleating effect of CaCO<sub>3</sub> nanoparticles, which resulted in spherulitic size reduction as nanofiller content increased. Using Scherrer equation [38], crystallite size was calculated from the values of full width at half maximum for peak  $2\theta = 16.6^\circ$  and  $K = 0.94$ . The crystallite size was found to be 0.38 and 0.27nm respectively for NC-0 and NC-3. It was reported by Friedrich [39] that semi crystalline polymer with small spherulites tends to be tougher than that of coarse spherulites. This was attributed to the weak boundaries of larger spherulites when compared to small spherulites. In NC-3, spherulites formed were smaller in size due to nucleating effect of nano CaCO<sub>3</sub>, which enhanced the polymer-particle boundaries, leading to the increase in the toughness of nanocomposites. Further, nanoparticles such as CaCO<sub>3</sub> act as stress concentrators and promote cavitation at the polymer-particle boundaries. As a result, numerous cavitation sites were created at the interface between CaCO<sub>3</sub> particles and amorphous layers. The formed cavities were believed to release plastic constraint in the matrix and trigger large scale plastic deformation, leading to improvement in toughness.

**Table 2: Mechanical Properties of PLA Nanocomposites**

Sample Code	Tensile Strength (MPa)	Tensile Modulus (GPa)	Elongation at Break (%)	Flexural Strength (MPa)	Impact Strength (J/m)
NC-0	33.2	2.93	1.4	45.6	15
NC-0.25	40.4	3.27	1.4	48.1	17
NC-0.5	46.7	3.32	1.6	57.8	19
NC-1	50.6	3.35	2.6	77.2	25
NC-2	50.4	3.33	2.3	62.0	26
NC-3	43.6	3.31	1.6	51.8	29



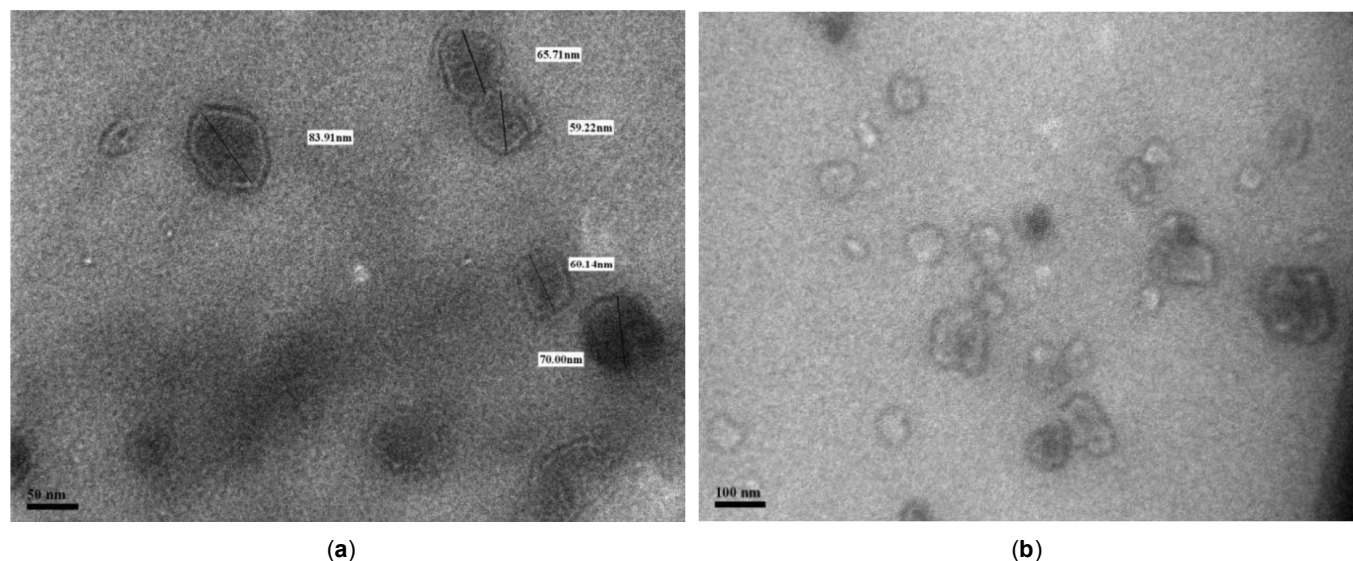


**Figure 5:** Transmission electron micrographs of; (a) NC-1 and (b) NC-3.

### 3.7. TEM Studies

TEM micrographs of ultra microtomed thin sections of NC-1 and NC-3 were obtained and are shown in Figure 5. The size of nanoCaCO<sub>3</sub> particles were found to be in the range of 59.2 to 83.9 nm in nanocomposites as observed from the TEM images. Further, TEM micrograph of NC-1 also revealed that a better dispersion was obtained when compared to that of NC-3. Better dispersion in NC-1 was reflected in improvement of HDT, tensile and flexural properties over NC-0 and the marginal improvement of these properties in the case of NC-3 was due to the agglomeration of nanoparticles.

### 3.8. Thermal Stability

Thermal stability of nanocomposites was evaluated in nitrogen atmosphere using TGA. The TGA data values are tabulated in Table 3. Both pristine PLA and nanocomposite samples were stable up to 300°C and showed single step degradation. Based on the 5% weight loss values, one can conclude that thermal stability decreased with increase in nanofiller content. The basic nature of CaCO<sub>3</sub> might catalyze the depolymerization of ester bonds of PLA, which reduce thermal stability [40]. Percent residue increased with increase in nanofiller content.

Coats-Redfern [41] method was used to determine the activation energy for thermal degradation of nanocomposites and the equation used is given below:

$$\ln \left[ \frac{-\ln(1-\alpha)}{T^2} \right] = \ln \left( \frac{AR}{\phi E_a} \right) \left[ 1 - \left( \frac{2RT}{E_a} \right) \right] - \left( \frac{E_a}{RT} \right)$$

where  $\alpha$  is the fraction decomposed at temperature  $T$ ,  $\phi$  is the heating rate,  $E_a$  is the activation energy for thermal decomposition reaction,  $R$  is the universal gas constant and  $A$  is the Arrhenius frequency factor. When the order of reaction is one, then the plot of  $\ln[-\ln(1-\alpha)/T^2]$  vs.  $1/T$  gives a straight line with slope equivalent to  $-E_a/R$ . Plot of  $\ln[-\ln(1-\alpha)/T^2]$  vs.  $1/T$  gave a straight line suggesting that decomposition followed first order kinetics in nitrogen atmosphere. Activation energy calculated from the slope of these curves is given in Table 3. Activation energy for thermal degradation of nanocomposites was found to be higher than pristine PLA (NC-0). Both activation energy and frequency factor increased with increase in nanofiller content. The ratio of  $E_a / \ln A$  was used to characterize the thermal stability of nanocomposites. The lower ratio of  $E_a / \ln A$  indicates lower thermal stability [28]. The calculated ratio values are given in Table 3. On comparing the values of  $E_a / \ln A$  ratio of nanocomposites, it was concluded that the thermal stability decreased with increase in nanofiller content and this is in corroboration with the weight loss data.

**Table 3: TGA data of PLA Nanocomposites**

Sample Code	T <sub>5</sub> (°C)	Residue (%)	E <sub>a</sub> (kJ/mol)	ln A (min <sup>-1</sup> )	E <sub>a</sub> /ln A
NC-0	323	0	170.6	18.57	9.19
NC-0.5	311	0.45	173.3	19.72	8.79
NC-2	311	1.67	189.5	22.96	8.25
NC-3	311	3.21	191.5	23.21	8.23

## CONCLUSIONS

We have successfully prepared PLA–nanoCaCO<sub>3</sub> nanocomposites by melt blending technique. Nano CaCO<sub>3</sub> was found to be promising nanofiller to overcome the limitations of PLA such as low HDT, water absorption and impact strength.

## REFERENCES

- [1] Mehta R, Kumar V, Bhunia H and Upadhyay S. Synthesis of poly (lactic acid): a review. *J Macromol Sci Polym Rev* 2005; 45: 325-49. <https://doi.org/10.1080/15321790500304148>
- [2] Drumright RE, Gruber PR and Henton DE. Poly(lactic acid) technology. *Adv Mater* 2000; 12: 1841-46. [https://doi.org/10.1002/1521-4095\(200012\)12:23<1841::AID-ADMA1841>3.0.CO;2-E](https://doi.org/10.1002/1521-4095(200012)12:23<1841::AID-ADMA1841>3.0.CO;2-E)
- [3] Garlotta RA. A literature review of poly(lactic acid). *J Polym Environ* 2001; 9 (2): 63-84. <https://doi.org/10.1023/A:1020200822435>
- [4] Lim LT, Auras R and Rubino M. Processing technologies for poly (lactic acid). *Prog Polym Sci* 2008; 33: 820-52. <https://doi.org/10.1016/j.progpolymsci.2008.05.004>
- [5] Sodergard A and Stolt M. Properties of lactic acid based polymers and their correlation with composition. *Prog Polym Sci* 2002; 27: 1123-63. [https://doi.org/10.1016/S0079-6700\(02\)00012-6](https://doi.org/10.1016/S0079-6700(02)00012-6)
- [6] Nampoothiri KM, Nair NR and John RP. An overview of the recent developments in polylactide (PLA) research. *Bioresour Technol* 2010; 101: 8493-8501. <https://doi.org/10.1016/j.biortech.2010.05.092>
- [7] NatureWorks ingeo: Naturally advanced materials. Ingeo Joins European Bio plastics Conference for the Third Edition. <http://www.natureworksilc.com/News-and-Events/Press-Releases/2008/10-30-08-EUBioplasticsConf.> (September 12, 2016).
- [8] Jamshidian M, Tehrani EA, Imran M, Jacquot M and Desobry S. Poly lactic acid: production, applications, nanocomposites, and release studies. *Compr Rev Food Sci Food Saf* 2010; 9: 552-71. <https://doi.org/10.1111/j.1541-4337.2010.00126.x>
- [9] Park JW and Im SS. Phase behavior and morphology in blends of poly(L-lactic acid) and poly(butylene succinate) *J Appl Polym Sci* 2002; 86: 647-55. <https://doi.org/10.1002/app.10923>
- [10] Na YH, He Y, Shuai X, Kikkawa Y, Doi Y and Inoue Y. Compatibility effect of poly(ε-caprolactone)-*b*-poly(ethylene glycol) block copolymers and phase morphology analysis in immiscible poly(lactide)/ poly(ε-caprolactone) blends. *Biomacromolecules* 2002: 1179-86. <https://doi.org/10.1021/bm020050r>
- [11] Hu Y, Hu YS, Topolkaev V, Hiltner A and Baer E. Crystallization and phase separation in blends of high stereo regular poly(lactide) with poly(ethylene glycol). *Polymer* 2003; 44: 5681-9. [https://doi.org/10.1016/S0032-3861\(03\)00609-8](https://doi.org/10.1016/S0032-3861(03)00609-8)
- [12] Gajria AM, Dave V, Gross RA and McCarthy SP. Miscibility and biodegradability of blends of poly(lactic acid) and Poly(vinyl acetate). *Polymer* 1996; 37: 437-44. [https://doi.org/10.1016/0032-3861\(96\)82913-2](https://doi.org/10.1016/0032-3861(96)82913-2)
- [13] Ishida S, Nagasaki R, Chino K, Dong T and Inoue Y. Toughening of poly(L-lactide) by melt blending with rubbers. *J Appl Polym Sci* 2009; 113: 558-66. <https://doi.org/10.1002/app.30134>
- [14] Balakrishnan H, Hassan A, Wahit S and Yussuf AA. Novel toughened polylactic acid nanocomposite: mechanical, thermal and morphological properties. *Mater Des* 2010; 31: 3289-298. <https://doi.org/10.1016/j.matdes.2010.02.008>
- [15] Jiang L, Wolcott MP and Zhang J. Study of biodegradable polylactide / poly(butylene adipate-co-terephthalate) blends. *Biomacromolecules* 2006; 7:199-207. <https://doi.org/10.1021/bm050581g>
- [16] Kulinski Z, Piorkowska E, Gadzinowska K. Plasticization of poly(L-lactide) with poly(propylene glycol). *Biomacromolecules* 2006; 7(7): 2128-2135. <https://doi.org/10.1021/bm060089m>
- [17] Martin O and Averous L. Poly(lactic acid): Plasticization and properties of biodegradable multiphase systems. *Polymer* 2001; 42: 6209-6219. [https://doi.org/10.1016/S0032-3861\(01\)00086-6](https://doi.org/10.1016/S0032-3861(01)00086-6)
- [18] Labrecque LV, Kumar RA, Dave V, Gross RA and McCarthy SP. Citrate esters as plasticizers for poly(lactic acid). *J Appl Polym Sci* 1997; 66: 1507-13. [https://doi.org/10.1002/\(SICI\)1097-4628\(19971121\)66:8<1507::AID-APP11>3.0.CO;2-O](https://doi.org/10.1002/(SICI)1097-4628(19971121)66:8<1507::AID-APP11>3.0.CO;2-O)
- [19] Ljungberg N, Andersson T and Wesslen B. Film extrusion and film weld ability of poly(lactic acid) plasticized with triacetin and tributyl citrate. *J Appl Polym Sci* 2003; 88: 3239-46. <https://doi.org/10.1002/app.12106>
- [20] Ljungberg N and Wesslen B. The effects of plasticizers on the dynamic mechanical and thermal properties of poly(lactic acid). *J Appl Polym Sci* 2002; 86: 1227-34. <https://doi.org/10.1002/app.11077>
- [21] Ljungberg N and Wesslen B. Preparation and properties of plasticized poly(lactic acid) films. *Biomacromolecules* 2005; 6: 1789-96. <https://doi.org/10.1021/bm050098f>
- [22] Jacobsen S and Fritz HG. Plasticizing polylactide - the effect of different plasticizers on the mechanical properties. *Polym Eng Sci* 1999; 39: 1303-10. <https://doi.org/10.1002/pen.11517>
- [23] Shibata M, Someya Y, Orihara M and Miyoshi M. Thermal and mechanical properties of plasticized poly (L-lactide) nanocomposites with organo-modified montmorillonites. *J Appl Polym Sci* 2006; 99: 2594-2602. <https://doi.org/10.1002/app.22268>
- [24] Hasook A, Tanoue S and Iemoto Y. Characterization and mechanical properties of poly(lactic acid) / poly(ε-caprolactone) / organo clay nanocomposites prepared by melt compounding. *Polym Eng Sci* 2006; 46: 1001-07. <https://doi.org/10.1002/pen.20579>
- [25] Murariu M, Ferreira AD, Degee P, Alexandre M and Dubois P. Poly(lactide) compositions. Part 1: Effect of filler content and size on mechanical properties of PLA/calcium sulfate composites. *Polymer* 2007; 48: 2613-8. <https://doi.org/10.1016/j.polymer.2007.02.067>
- [26] Jiang L, Zhang J and Wolcott MP. Comparison of polylactide /nanosized calcium carbonate and polylactide/ montmorillonite composites; reinforcing effects and toughening mechanisms. *Polymer* 2007; 48: 7632-44. <https://doi.org/10.1016/j.polymer.2007.11.001>
- [27] Liang JZ, Zhou L, Tang CY and Tsui CP. Crystalline Properties of poly(L-lactic acid) composites filled with nanometer calcium carbonate. *Composites Part B* 2013; 45: 1646-1650. <https://doi.org/10.1016/j.compositesb.2012.09.086>
- [28] Andricic B, Kovacic T, Perinovic S and Grgic A. Thermal properties of poly(L-lactide) / calcium carbonate nanocomposites. *Macromol Symp* 2008; 263: 96-101. <https://doi.org/10.1002/masy.200850312>
- [29] Navarro M, Engel E, Planell JA, Amaral I, Barbosa M and Ginebra MP. Surface characterization and cell response of a PLA / CaP glass biodegradable composite material.

- J Biomed Mater Res 2008; 85: 477-86.  
<https://doi.org/10.1002/jbm.a.31546>
- [30] Maurya SD, Purushothaman M, Krishnan PSG and Nayak SK. Effect of nano-calcium carbonate content on the properties of poly(urethane methacrylate) nanocomposites J Thermoplast Comp Mater 2013; 27: 1711-27.
- [31] Lin Y, Chen H, Chan CM and Wu J. Nucleating effect of calcium stearate coated CaCO<sub>3</sub> nanoparticles on polypropylene. J Colloid Interface Sci 2011; 354: 570-576.  
<https://doi.org/10.1016/j.jcis.2010.10.069>
- [32] Wang M, Lin L, Peng Q, Ou W and Li H. Crystallization and mechanical properties of isotactic polypropylene/calcium carbonate nanocomposites with a stratified distribution of calcium carbonate. J Appl Polym Sci 2014; 131: 39632.  
<https://doi.org/10.1002/app.39632>
- [33] Chan CM, Wu J, Li JX and Cheung YK. Polypropylene / calcium carbonate nanocomposites. Polymer 2002; 43: 2981-2992.  
[https://doi.org/10.1016/S0032-3861\(02\)00120-9](https://doi.org/10.1016/S0032-3861(02)00120-9)
- [34] Wu MT and Wu CY. Biodegradable poly(lactic acid)/chitosan-modified montmorillonite nanocomposites: Preparation and characterization. Polym Degrad Stab 2006; 91: 2198-2204.  
<https://doi.org/10.1016/j.polymdegradstab.2006.01.004>
- [35] Nam YJ, Ray SS and Okamoto M. Crystallization behavior and morphology of biodegradable polylactide/layered silicate nano composite. Macromolecules 2003; 36: 7126-31.  
<https://doi.org/10.1021/ma034623j>
- [36] Das K, Ray D, Banerjee I, Bandyopadhyay NR, Sengupta S, Mohanty AK, et al. Crystalline morphology of PLA/clay nano composite films and its correlation with other properties. J Appl Polym Sci 2010; 118: 143-151.  
<https://doi.org/10.1002/app.32345>
- [37] Cenna AA, Doyle J, Page NW, Beehag A and Dastoor P. Wear mechanisms in polymer matrix composites abraded by bulk solids. Wear 2000; 240: 207-214.  
[https://doi.org/10.1016/S0043-1648\(00\)00365-3](https://doi.org/10.1016/S0043-1648(00)00365-3)
- [38] Revol JF, Dietrich A and Goring DAI. Effect of mercerization on the crystallite size and crystallinity index in cellulose from different sources. J Chem 1987; 65: 1724-1725.  
<https://doi.org/10.1139/v87-288>
- [39] Friedrich K. Crazes and shear bands in semicrystalline thermoplastics Adv Polym Sci 1983; 52: 225-274.  
<https://doi.org/10.1007/BFb0024059>
- [40] Kim HS, Park BH, Choi JH and Yoon JS. Mechanical properties and thermal stability of poly(L-lactide)/calcium carbonate composites. J Appl Polym Sci 2008; 109: 3087-3092.  
<https://doi.org/10.1002/app.28229>
- [41] Coats A and Redfern JP. Kinetic parameters from thermo gravimetric data. Natur 1964; 201: 68-69.  
<https://doi.org/10.1038/201068a0>

Received on 26-11-2016

Accepted on 18-01-2017

Published on 23-10-2017

DOI: <https://doi.org/10.12974/2311-8717.2017.05.01.4>© 2017 Pundir *et al.*; Licensee Savvy Science Publisher.

This is an open access article licensed under the terms of the Creative Commons Attribution Non-Commercial License (<http://creativecommons.org/licenses/by-nc/3.0/>) which permits unrestricted, non-commercial use, distribution and reproduction in any medium, provided the work is properly cited.